

# A PAIR PLASMA MODEL FOR PKS 0208–512

I.V. Moskalenko<sup>1,2</sup>, W.Collmar<sup>1</sup>

- 1) *Max-Planck-Institut für extraterrestrische Physik, D-85740 Garching, Germany*
- 2) *Institute for Nuclear Physics, Moscow State University, 119 899 Moscow, Russia*

**ABSTRACT** Assuming that the enhanced MeV emission from the MeV blazar PKS 0208–512 observed by COMPTEL on occasions is due to annihilation in a pair plasma, we estimate parameters of the annihilation region: its size, the number density of particles, and the variability timescale. The values we find are in accord with our present-day knowledge of emission mechanisms operating in AGNs. The constructed model implies that the blueshifted annihilation emission is an intrinsic property of all AGN jet models, and predicts an anticorrelation between the high-energy emission and the annihilation flux.

**KEYWORDS:** galaxies: active; BL Lac objects: individual (PKS 0208–512); gamma rays: theory.

## 1. INTRODUCTION

During six years of operation about 70 blazars have been detected by the EGRET telescope at  $\geq 100$  MeV (e.g., Hartman et al. 1997). Although the origin of the blazar  $\gamma$ -ray emission is still discussed, the inverse Compton scattering of soft photons off relativistic electrons in a collimated jet is widely accepted (e.g., Dermer et al. 1992, Maraschi et al. 1992). Other models associate the  $\gamma$ -ray emission with  $\pi^0$ -production by relativistic nucleons (e.g., Mastichiadis & Protheroe 1990, Mannheim 1993).

COMPTEL observations indicate a class of  $\gamma$ -ray blazars which display spectral energy distributions peaking in a narrow energy band at a few MeV (Bloemen et al. 1995, Blom et al. 1995, 1996). The blazar PKS 0208–512 was detected in the analysis of COMPTEL data by Blom et al. (1995). The signal was obtained by combining data from May 8–13, 1993 and June 3–14, 1993, yielding a strong flux in the 1–3 MeV band, and only upper limits at lower and higher COMPTEL energies. Contemporary observations with EGRET yielded a significant detection above 100 MeV. The peak in the  $\nu F_\nu$  spectrum of PKS 0208–512 occurs at MeV energies (Kanbach 1996). Remarkable is the anticorrelation in the source flux at COMPTEL and EGRET energy ranges for the CGRO Phases I and II.

The MeV features observed by COMPTEL can not be explained in the framework of jet-scattered background emission and therefore probably have a different origin. The most natural one seems the interpretation of Doppler boosted  $e^+e^-$ -annihilation radiation (e.g., Henri et al. 1993, Roland & Hermsen 1995). The clear and pronounced feature observed from PKS 0208–512 allows model fitting accurate enough to derive such parameters as the pair plasma temperature, the bulk

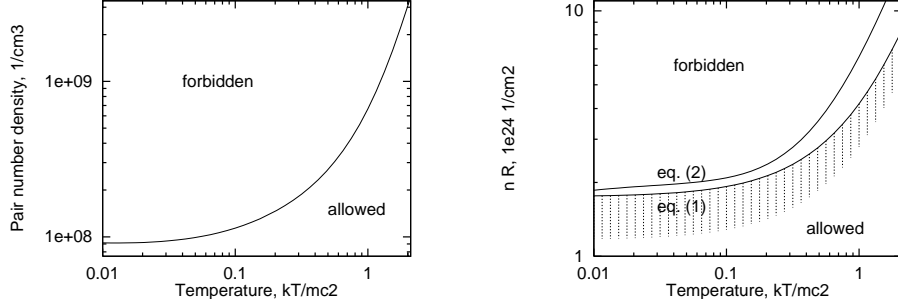


FIGURE 1. Left: The upper limit for pair number density (eq. [1]),  $L_a^* = 10^{46} \text{ erg s}^{-1}$ . Right: The upper limits for the product  $(n_{\pm}^* R^*)$  vs. plasma temperature.

Lorentz factor, viewing angle, and the intrinsic annihilation luminosity (Skibo et al. 1997); it has also been shown that the existence of a class of MeV blazars can be understood by orientation effects, and is consistent with AGN unification scenarios.

## 2. ANNIHILATION OF THE THERMAL PAIR PLASMA

A distinct annihilation line from a pair plasma can only be observed if the plasma is optically thin. The opacity of an optically thin pair plasma is dominated by Compton scatterings. We thus consider only the case when the Compton scattering optical depth is less than unity  $\tau_C(\theta) = 2n_{\pm}^* R^* \sigma_{KN}(\theta) \leq 1$ , where  $n_{\pm}^*$  is the number density of pairs,  $R^*$  is the radius of the plasma blob,  $\sigma_{KN}(\theta) \approx \sigma_{KN}(\theta; \epsilon_{\max})$  is the Klein-Nishina cross section averaged over the thermal electron distribution,  $\theta = kT/mc^2$  is the plasma temperature, and  $\epsilon_{\max}$  is the energy of the center of the annihilation line. An asterisk marks variables in the comoving frame.

The annihilation luminosity can be obtained as  $L_a^* = 4\pi c R^{*2} t_{esc} \langle \dot{n} \epsilon \rangle$ , where  $t_{esc} \sim R^*/c$  is the photon escape time in the optically thin plasma, and the annihilation emissivity is given by  $\langle \dot{n} \epsilon \rangle \approx 2\pi r_e^2 c n_{\pm}^{*2} A(\theta) \bar{\epsilon}$ . Here the factor of 2 accounts for 2 photons per annihilation event,  $r_e$  is the classical electron radius,  $\bar{\epsilon} \sim \epsilon_{\max}$  is the average energy of the annihilation photon,  $A(\theta)$  is the dimensionless annihilation rate (Moskalenko & Jourdain 1997) averaged over the thermal pair distribution, and  $t_a^* = [\pi r_e^2 c n_{\pm}^* A(\theta)]^{-1}$  is the intrinsic annihilation timescale.

The condition  $\tau_C \leq 1$  yields estimates for the pair density and the blob radius

$$n_{\pm}^* \leq \pi^2 r_e^2 c A(\theta) \bar{\epsilon} / [\sigma_{KN}^3(\theta) L_a^*], \quad n_{\pm}^* R^* \leq [2\sigma_{KN}(\theta)]^{-1}, \quad (1)$$

which depend only on the luminosity  $L_a^*$  and the plasma temperature. Converting  $t_a^*$  into the blob size by using the light travel time  $2R^* \leq ct_a^*$  yields another estimate,

$$n_{\pm}^* R^* \leq [2\pi r_e^2 A(\theta)]^{-1}. \quad (2)$$

The upper limits for  $n_{\pm}^*$  and  $(n_{\pm}^* R^*)$  are shown in Fig. 1. Expr. (1)–(2) agree better than a factor of 2, showing that the variability timescale in the comoving frame is approximately twice the intrinsic annihilation timescale,  $\Delta_d^* \sim 2t_a^*$ .

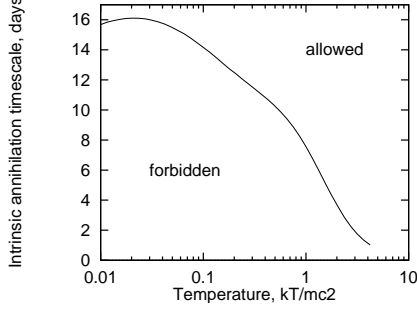


FIGURE 2. The intrinsic annihilation timescale,  $t_a^*(\theta)$ , for  $L_a^* = 10^{46}$  erg s $^{-1}$ .

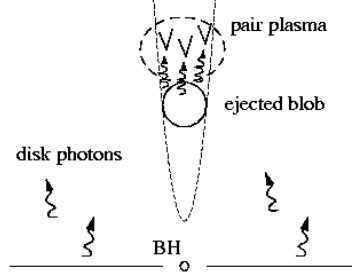


FIGURE 3. Schematic view illustrating the model.

These formulae allow the derivation of a lower limit on the observed variability timescale of the annihilation line from a single pair plasma blob ( $\tau_C \leq 1$ ):

$$\Delta_d = \frac{1+z}{\mathcal{D}} \frac{3t_a^*}{2} \geq \frac{1+z}{\mathcal{D}} \frac{3\sigma_{KN}^3(\theta) L_a^*}{2\pi\bar{\epsilon} [\pi r_c^2 c A(\theta)]^2}, \quad (3)$$

where  $z$  is the redshift, and  $\mathcal{D}$  is the Doppler factor, and we took also into account that the variation timescale in  $L_a^*$  should be a factor of 2 shorter than  $t_a^*$  ( $\dot{L}_a/L_a = 2\dot{n}_\pm/n_\pm$ ). The intrinsic annihilation timescale,  $t_a^*(\theta)$ , is shown in Fig. 2.

Since the annihilation line from the pair plasma blob is most effectively emitted when  $\tau \sim 1$ , the pair number density is most probably equal to its upper limit (eq. [1]). Thus the blob radius is  $R^* \sim [2n_\pm^* \sigma_{KN}(\theta)]^{-1}$ , and the variability timescale should be close to its lower limit (eq. [3]).

Assuming that the enhanced MeV emission observed from PKS 0208–512 is due to annihilation in the outflowing thermal pair plasma blob, we adopt the parameters obtained by Skibo et al. (1997) from the spectral fitting:  $L_a^* = 3.3 \times 10^{46}$  erg s $^{-1}$ ,  $\theta = 0.5$ , a bulk Lorentz factor  $\Gamma = 3$ , and a viewing angle  $\psi = 18^\circ$ .

Eq. (1) allows to put the upper limit on the pair number density of the plasma blob as  $n_\pm^* \leq 8.2 \times 10^7$  cm $^{-3}$  (Fig. 1 left). The obtained variability timescale,  $\Delta_d \geq 31.5$  days ( $z = 1$ ,  $\mathcal{D} \approx 3.2$ ), agrees well with the total duration of 38 days (VPs 220.0, 224.0, + time in between) for which COMPTEL observed this MeV feature from PKS 0208–512. Using the upper limit,  $n_\pm^* \sim 8.2 \times 10^7$  cm $^{-3}$ , provides an estimate for the radius of  $R^* \sim 3.4 \times 10^{16}$  cm assuming the best observability conditions (see Fig. 1 right). This is a typical estimate for the blob radius (Dermer et al. 1997). The blob size  $d^* \sim c\Delta_0\mathcal{D}/(1+z) \approx 3.34 \times 10^{16}$  cm inferred from the shortest variability timescale of PKS 0208–512 observed by EGRET ( $\Delta_0 \approx 8$  days, von Montigny et al. 1995) matches well the above estimate for  $R^*$ . The annihilation timescale (eq. [3]) provides us also with a lower limit for the high energy emission site, which due to the  $\gamma\gamma$ -transparency arguments should be located at the distance of  $z_i \geq \Gamma c \frac{t_a^*}{2} \approx 0.01$  pc ( $\Gamma/3$ ) ( $L_a^*/3.3 \times 10^{46}$  erg s $^{-1}$ ) from the central engine.

### 3. THE MODEL

The  $\gamma\gamma$ -opacity effects play an important role when considering the generation of high energy  $\gamma$ -ray emission. In the early stage of the flare when the ejected plasma blob is still close to the central engine, it is embedded in a dense background radiation field. A huge optical depth due to the  $\gamma\gamma$ -pair production prevents the high energy photons from escaping. The pairs appear preferentially ahead of the ejected blob and move with relativistic speed in the same direction as follows from the energy-momentum conservation law (Fig. 3). A relatively small Lorentz factor of the pairs and large optical depth of the pair plasma itself makes it easier to establish (quasi-) thermal equilibrium. The annihilation of pairs gives rise to annihilation photons, for which the background radiation field is transparent. The annihilation line becomes visible as soon as the optical depth of the pair plasma cloud becomes less than unity while its size is large enough to produce the observed flux. The high energy  $\gamma$ -ray emission appears when the plasma blob/jet is already far from the central engine, since  $\gamma\gamma$  absorption on background photons is negligible and the pair plasma ahead also becomes too rare due to annihilation and/or spatial expansion.

Generation and annihilation of a pair plasma should thus be an intrinsic property of all relativistic blob/jet models. However, the detection of the annihilation line depends on its luminosity and viewing angle (Skibo et al. 1997). The described model provides support to models which include two populations of jet particles, although the exact flow geometry is still unknown. According to our model, the annihilation feature should appear before the high energy radiation producing a visible anticorrelation on a timescale of  $\Delta_d$  (eq. [3]); this matches the observations of PKS 0208–512 where the anticorrelation has been noted (Blom et al. 1996).

### REFERENCES

- Bloemen, H., et al. 1995, *A&A*, 293, L1  
Blom, J.J., et al. 1995, *A&A*, 298, L33  
Blom, J.J., et al. 1996, *A&AS*, 120C, 507  
Dermer, C.D., Schlickeiser, R., Mastichiadis, A. 1992, *A&A*, 256, L27  
Dermer, C.D., Sturmer, S.J., Schlickeiser, R. 1997, *ApJS*, 109, 103  
Hartman, R.C., et al. 1997, in 4th Compton Symp. AIP 410, AIP, New York, p.307  
Henri, G., Pelletier, G., Roland, J. 1993, *ApJ*, 404, L41  
Kanbach, G. 1996, in Workshop on Gamma-ray emitting AGN, MPI H-V37-1996, Heidelberg, p.1  
Maraschi, L., Ghisellini, G., Celotti, A. 1992, *ApJ*, 397, L5  
Mannheim, K. 1993, *A&A*, 269, 67  
Mastichiadis, A., Protheroe, R.J. 1990, *MNRAS*, 246, 279  
von Montigny, C., et al. 1995, *ApJ*, 440, 525  
Moskalenko, I.V., Jourdain, E. 1997, *A&A*, 325, 401  
Roland, J., Hermesen, W. 1995, *A&A*, 297, L9  
Skibo, J.G., Dermer, C.D., Schlickeiser R. 1997, *ApJ*, 483, 56